Physics – Uspekhi **45** (11) 1165 – 1174 (2002)

METHODOLOGICAL NOTES PACS numbers: **71.23. – k**, **71.30. + h**, 72.15.Rn

Chemical localization

V F Gantmakher

DOI: 10.1070/PU2002v045n11ABEH001246

Contents

Abstract. The possibility that, in spite of high valence electron concentrations, metal – insulator transitions can in principle occur in materials composed of atoms of only metallic elements is demonstrated based on the analysis of experimental data. For such a transition to occur, stable atomic configurations forming deep potential wells capable of trapping dozens of valence electrons should appear in the system. This means, in essence, that bulk metallic medium transforms into an assembly of identical quantum dots. Depending on the parameters, such a material either does contain delocalized electrons (metal) or does not contain such electrons (insulator). The degree of disorder is one of these parameters. Two types of substances with such properties are discussed: liquid binary alloys with both components being metallic, and thermodynamically stable quasicrystals.

1. Introduction

The band theory of metals, with its concept of energy-band overlap, describes rather than explains the metallic properties of matter. The fundamental reason for the existence of the metallic state is that in an isolated metal atom the valence electrons occupy positions close to the upper edge of the potential well, so that in the condensed state any perturbation introduced by neighboring metal atoms leads to delocalization of the valence electrons. From this viewpoint, the grouping of chemical elements into metals and metalloids is caused by the atomic structure; metals are in the lower left corner of the Periodic Table, and the boundary between metals and metalloids, which is a diagonal of the Periodic Table, is blurred and extremely conventional. The transport properties of chemical substances and substances that are a mixture of metal and metalloid atoms depend on various factors. By selecting one of these factors as the driving parameter, we can initiate a metal – insulator transition.

The most common model describing a metal – insulator transition is the Anderson model [1] in which disorder is the cause of the transition. The model examines a periodic lattice of rectangular wells of different depths. The energy levels in the wells are within an interval of values W, and the level density in this interval is assumed constant. Thanks to the tails of the wave functions, $\exp(-r/\lambda)$, there is an overlap of the wave functions of the electrons localized in neighboring wells. If the distance between the neighboring wells, r_{12}, is much larger than λ, the overlap integral

$$J \sim \int \psi_1^* \hat{H} \psi_2 \, \mathrm{d}^3 r \sim J_0 \exp\left(-\frac{r_{12}}{\lambda}\right) \tag{1}$$

is small, with the smallness determined by the factor $\exp(-r_{12}/\lambda)$. The quantity λ is often called the Bohr radius, by analogy with the hydrogen atom.

Two limits are possible here. Each electron may occupy its own well — this is the case for very deep but different wells. On the other hand, all electrons may be delocalized, so that any electron may find itself in any well. For instance, if all the wells are the same or almost the same, the electron wave functions are simply Bloch waves.

The ratio of two energies, the width of the band W and the overlap integral J, acts as a parameter in this problem. What Anderson stated was that for delocalized states to emerge, i.e. for metallic conductivity to set in, the following condition must be met:

$$\frac{J}{W} \geqslant \left(\frac{J}{W}\right)_{\mathrm{crit}} . \tag{2}$$

When the ratio J/W is critical, delocalized states appear in the center of the band at $\epsilon = 0$; a further increase in J/W leads to a gradual 'thickening' of the layer of delocalized states.

Plugging the estimate (1) for the overlap integral into Eqn (2) and replacing r_{12} with the average distance between the centers, $n^{-1/3}$, we arrive at the following criterion for a transition to occur:

$$\lambda n^{1/3} = -\left(\ln \frac{c_{\mathrm{A}} W}{J_0}\right)^{-1}, \qquad c_{\mathrm{A}} = \left(\frac{J}{W}\right)_{\mathrm{crit}} . \tag{3}$$

V F Gantmakher Institute of Solid State Physics,
Russian Academy of Sciences,
142432 Chernogolovka, Moscow Region, Russian Federation
Tel. (7-096) 522 29 42. Fax (7-096) 524 97 01
E-mail: gantm@issp.ac.ru

Received 17 May 2002
Uspekhi Fizicheskikh Nauk **172** (11) 1283 – 1293 (2002)
Translated by E Yankovsky; edited by M V Magnitskaya

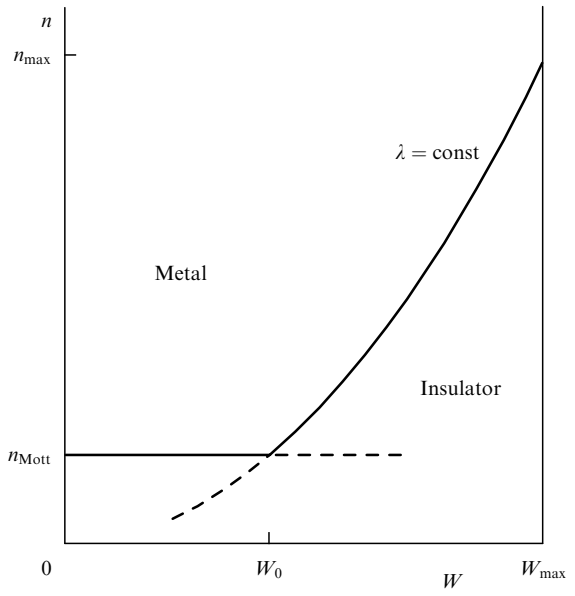

Figure 1. Diagram illustrating the possibility of an upper limit for electron concentrations that allow for an Anderson transition as disorder increases.

We select W as the measure of disorder and consider the (W, n) plane. Let us assume that the Bohr radius λ is constant. The disorder introduced into the system by atomic displacements has an upper limit. The limit is reached when there is no correlation between the positions of the atoms (we denote it by W_{max}). In this limit the whole plane of possible states is reduced to the region $0-W_{max}$ (see Fig. 1). The solid curve within this region is the transition curve (3), with insulator state to the right of the curve and metal state, to the left. The concentration n_{max} corresponds to the disorder W_{max} on the transition curve. But what are the electron concentrations n in real metals and alloys compared to n_{max}? If $n > n_{max}$, an Anderson transition cannot be initiated, no matter how great the disorder. Of course, W can be considered a quantitative measure of disorder only very conditionally. Hence the diagram in Fig. 1 is only an illustration. Nevertheless, the question exists and only experiments will provide an answer.

Not only disorder but also the electron – electron interaction may serve as the driving force for a metal – insulator transition. A transition initiated by such interaction is called 'Mott transition' [2]. What makes it so different from an Anderson transition is that it occurs at a fixed degree of disorder. When the number of metal atoms is very small, even if we were to align them inside an insulator to form a superlattice, so that there is no disorder, the substance still remains an insulator. It can become a metal only if we increase n. Actually, it is impossible to vary the electron concentration n and, at the same time, to keep the amplitude and the characteristic lengths of the random potential constant; it is also impossible to vary the parameters of the random potential and keep the concentration n constant. Hence usually it is impossible to distinguish between an Anderson transition and a Mott transition. However, the fact that there are two possible reasons for metal – insulator transitions should never be ignored.

The criterion of a Mott transition can easily be written in a form similar to (3):

$$\lambda n^{1/3} = -\left(\ln \frac{c_M U}{J_0}\right)^{-1}, \qquad (4)$$

the only difference being that instead of W we have the Hubbard energy U which describes the electrostatic repulsion of two electrons localized at one site, and instead of c_A we have a different numerical constant c_M. The Mott's transition curve (4) is represented in Fig. 1 by a straight horizontal line, and the smaller the value of λ the higher the line. The two lines, (3) and (4), intersect at the point $W_0 = (c_M/c_A)U$. As long as the disorder is large $(W > W_0)$, the metal – insulator transition is controlled by it and occurs along the curve (3). Small disorder $(W < W_0)$ does not play any role since localization is caused by the electron – electron interaction at concentrations n higher than those that follow from (3).

The metal – insulator transition has been realized in dozens of experiments. But all these experiments involved systems in which the metal atoms were diluted by nonmetal atoms which are not inclined to provide electrons for the general 'pool' (see Fig. 2, which has been taken from Ref. [3]). As techniques for fabricating amorphous metals (completely disordered materials based on metal alloys) developed, it seemed that metal – insulator transition would be discovered in them. However, even with the enormous diversity of such alloys, their resistivity never exceeds $\rho^* \approx 200-400$ μΩ cm [4].

For a given concentration n of carriers in the metal, $n = k_F^3/3\pi^2$, maximum resistance occurs when the mean free path l is at its minimum l_{min} which is expressed in terms of the Fermi wave vector k_F as $l_{min} \approx k_F^{-1}$. Then, to within

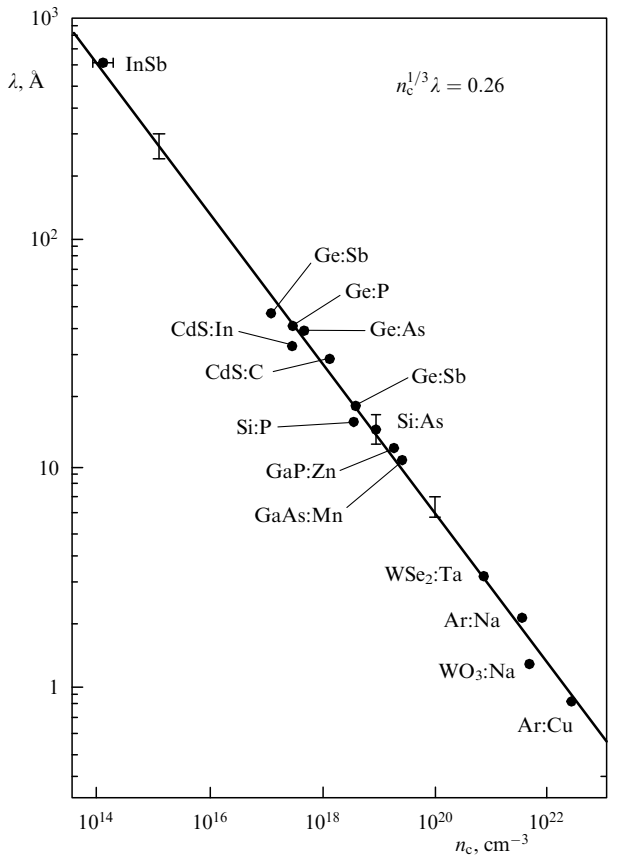

Figure 2. Correlation between the critical carrier concentration and the effective Bohr radius for the metal – insulator transitions that took place in 15 different materials. For all materials whose data were used in constructing this diagram, the values of λ and n_c were determined independently in different experiments [3].

numerical factors, we have

$$\rho = \frac{\hbar k_F}{ne^2 l} \simeq \frac{\hbar}{e^2}\, k_F^{-1} (k_F l)^{-1} \lesssim \rho^* \equiv \frac{\hbar}{e^2}\, k_F^{-1} = \frac{\hbar}{e^2}\, n^{-1/3}\,. \quad (5)$$

Assuming that the average atomic separation a in condensed matter is approximately 3 Å, we can introduce the electron concentration in a standard metal

$$n^* = a^{-3} \approx 4 \times 10^{22}\ \text{cm}^{-3}\,. \quad (6)$$

The maximum resistivity of a metal with such a carrier concentration is achieved with a mean free path $l \approx l_{\min}$ of order of the average distance $(n^*)^{-1/3}$ between the carriers and approximately equal to the de Broglie wavelength k_F^{-1}:

$$\rho^* \approx \frac{\hbar}{e^2}\, (n^*)^{-1/3} \approx (200-400)\ \mu\Omega\ \text{cm}\,. \quad (7)$$

The resistivity of almost all amorphous metals is just of the order of ρ^*. It occurs that in condensed media consisting only of metal atoms (they are called metal alloys) a rise in disorder does not by itself lead to localization. By introducing maximum disorder into the alloy we only bring it closer to the brink of localization. For the transition to occur, a fraction of the metal atoms must be replaced by metalloid atoms, which drives the concentration n of the delocalized electrons down to its critical value.

Injection of metalloid atoms can prove to be twice as effective in the sense that the concentration of metal atoms does not always uniquely determine the concentration n of the delocalized or potentially delocalizable electrons. If the metal and metalloid atoms can form stable chemical molecules, metal electrons leave for chemical bonds: from the shallow potential well of a metal atom they go to a much deeper potential well of the molecule and, therefore, remain localized, notwithstanding the surroundings of the molecule. Hence the effective electron concentration n, which affects the position of the material on the metal–insulator phase diagram, decreases even more due to the emergence of chemical bonds.

Bearing in mind the tying-up of a fraction of the potentially free valence electrons into chemical bonds, we can formulate the following question: *Is there a way to build deep potential wells, with only metal atoms on hand, which would transform a material that contains no metalloid atoms and must be a metal with the standard concentration* (6) *into an insulator?* The experimental data discussed in the present paper show that this is possible.

2. Intermetallic complexes in two-component melts

For a long time it has been known that the resistivity of a liquid melt of two very good metals may change severalfold, even by a factor of 10, depending on the relative concentration of the two components, and reach its maximum at a certain rational ratio of the atomic concentrations, such as 1 : 1, 1 : 3, or 1 : 4 [5, 6]. To gather such data, one must know how to measure the resistivity at a fixed temperature as a function of the alloy component concentration. A description of the respective experimental facilities can be found in Refs [7, 8].

Figure 3 shows the results of measurements of the resistivity of Na–Pb melts at 725 °C done by Calaway and Saboungi [8]. Clearly, the concentration ratio Na : Pb $\sim$ 4 : 1 is preferred. An addition of 20% of lead increases the resistivity compared to that of pure Na by a factor of about 20. Here the peak value of resistivity is of order of the maximum possible value ρ^* of a standard metal. The Li–Pb system behaves in a similar manner.

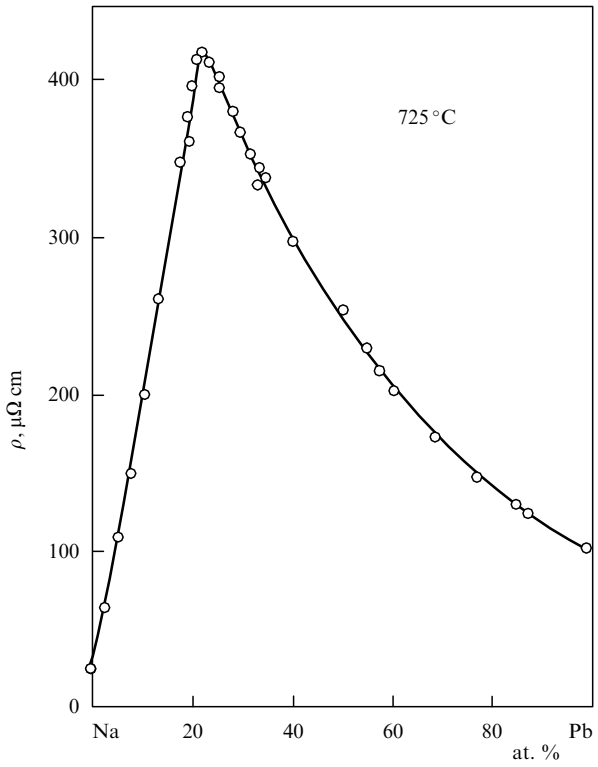

Figure 3. Resistivity of melts in the Na–Pb system at 725 °C. The peak value is reached at a lead concentration $C_{Pb} = 20\%$, where stable $PbNa_4$ configurations emerge [8].

Replacing Li and Na with a heavier alkali metal, K, Rb, or Cs, changes the concentration vs. resistivity diagram significantly. For example, Fig. 4 shows the diagram for the Rb–Pb system taken from Ref. [9]. The peak has shifted to another rational ratio of the component concentrations Rb : Pb $\sim$ 1 : 1, while the peak value of the resistivity increased severalfold. Now this value exceeds the maximum resistivity (7) of a standard metal (6) by a factor of 10. The survey diagrams in Fig. 5 show that melts of alkali metals with another tetravalent metal, tin, behave in the same manner [10]. Even higher resistivity values are realized in Cs-based melts.

The high values of resistivity mean that near the respective concentration ratios the melt ceases to be a standard metal, in the sense that a fraction of carriers in it are bound in some manner and the remaining effective concentration $n_{\text{eff}} \ll 4 \times 10^{22}\ \text{cm}^{-3}$ [cf. (6)]. Indeed, for the Rb–Pb system, the value $\rho \approx 2200\ \mu\Omega$ cm is about 10 times greater than the maximum value for a standard metal, $\rho^* \approx 200-400\ \mu\Omega$ cm. According to equations (5) and (7), this implies that the number of free carriers in the melt is no greater than $10^{-2}-10^{-3}$ of the ordinary number of carriers in a standard metal.

From the rational component-concentration ratios it follows that the increase in resistivity is due to formation of complexes within which most electrons prove to be locked.

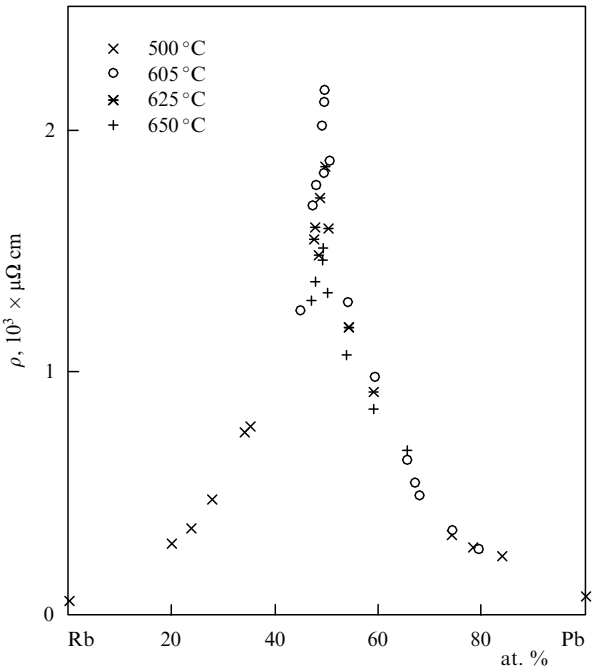

Figure 4. Resistivity of melts in the Rb – Pb system at different temperatures [9]. The peak value is reached at a lead concentration $C_{Pb} = 50\%$; the Pb_4Rb_4 configurations are stable.

The position of the peak in resistivity in Li- and Na-based melts unquestionably points to the existence of Na_4Pb and Li_4Pb complexes in the melts. The five atoms comprising such a complex have eight electrons in their valence shells. Apparently, they form a single stable outer shell of the Pb^{4-} ion, while four alkali ions held together by Coulomb forces

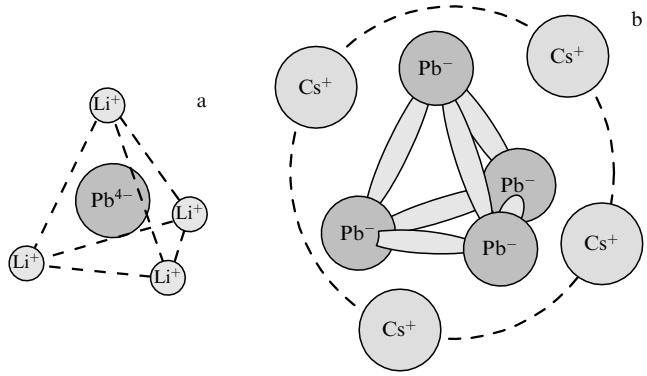

Figure 6. (a) Ionic configurations consisting of Pb or Sn atoms and a light alkali metal Li or Na; (b) the same with a heavy alkali metal K, Rb, or Cs.

are the surroundings of that ion. The four ions form a barrier thanks to which the eight electrons in the outer shell of Pb are kept within this electrically neutral atomic configuration and do not participate in conduction (Fig. 6a).

An increase in the size of the alkali atoms leads to a qualitative change in the forming complexes, with the ability of these complexes to act as electron traps gaining in strength. Such structures are well known and are called Zintl's structural units (named after the German chemist who, in the 1930s, discovered the rule of formation of ionic configurations [11]). If an electron goes from an alkali atom to the lead atom, the Pb^{1-} ion will have five electrons in the outer shell, the same as in the P or As atoms. As is known, in the gaseous phase these two elements form tetrahedral molecules P_4 or As_4. Here there are eight electrons near each atom of the molecule: five electrons belonging to the atom proper and one

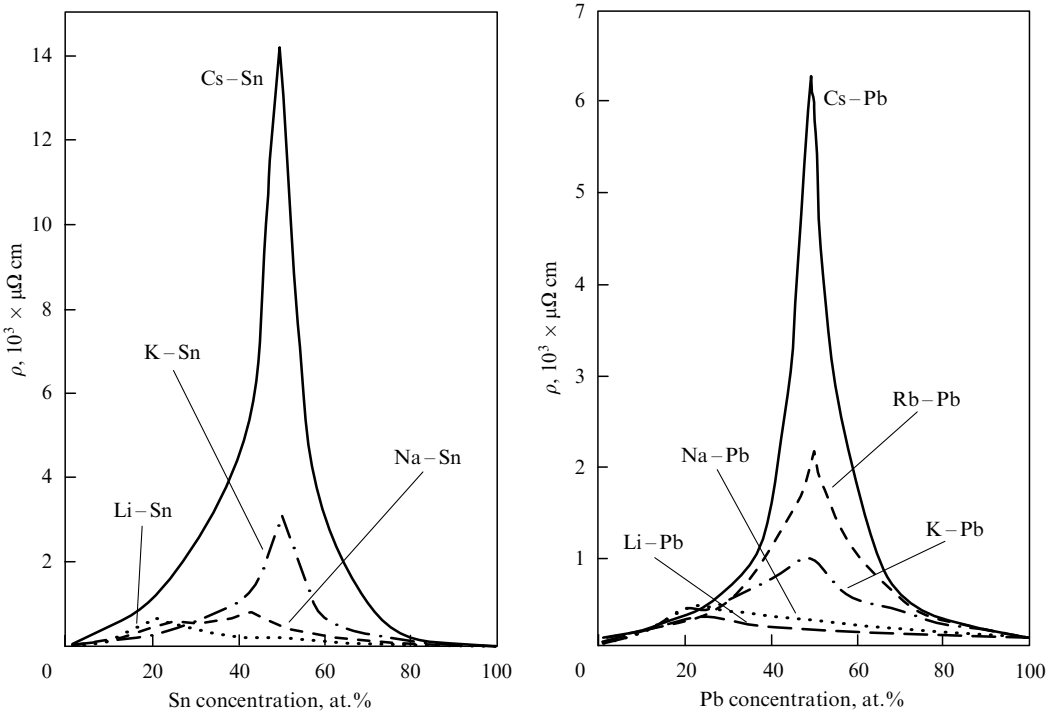

Figure 5. Survey diagrams of the resistivity vs. concentration dependence for melts of Sn – *B* and Pb – *B* systems (*B* is an alkali metal). The resistivity of alloys with Li and the Pb – Na alloy has a maximum at $C_A = 20\%$ (A = Pb, Sn); the resistivity of the Sn – Na alloy has two maxima at $C_{Sn} \approx 25\%$ and 45%; the rest have a resistivity maximum at $C_A = 50\%$ [10].

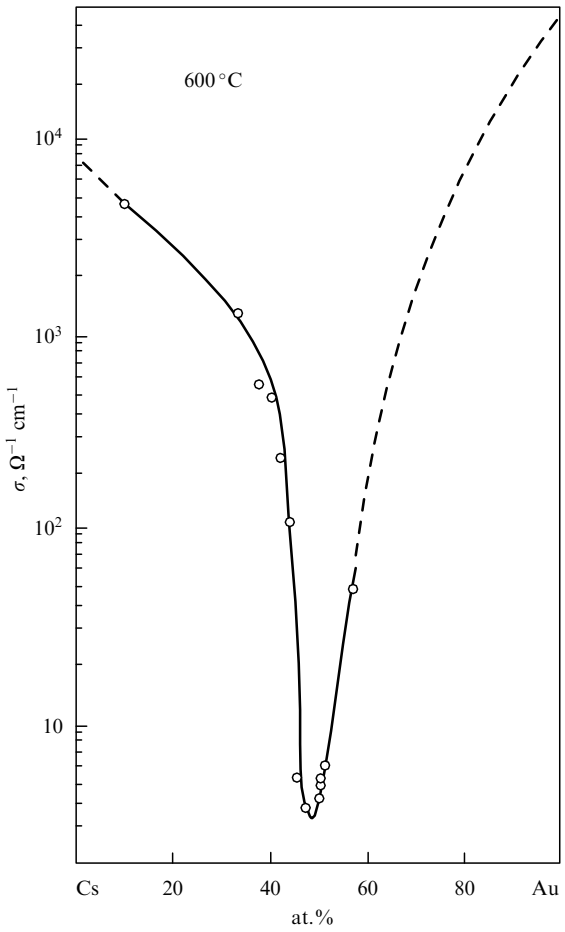

Figure 7. Conductivity of melts in the Cs–Au system at 600 °C [5, 12].

electron from the covalent bond of each of the three neighbors in the tetrahedron. Pb^{1-} ions also form such tetrahedrons, and the total electric charge $-4e$ of such a tetrahedron is balanced by the electric charge of the four alkali-metal ions surrounding it. Sn^{1-} ions form similar tetrahedrons $(Sn_4)^{4-}$ surrounded by four alkali ions. It is the structural unit

$$A_4B_4, \qquad A = \mathrm{Pb}, \mathrm{Sn}\,, \qquad B = \mathrm{K}, \mathrm{Rb}, \mathrm{Cs} \tag{8}$$

that is the configuration within which 20 valence electrons are locked (Fig. 6b).

Binary melts consisting of alkali metals and some other metals behave in a similar manner. The absolute champion when it comes to forming effective electron traps is the isoatomic melt of two ideal metals, the alkali metal Cs and the noble metal Au. As Fig. 7 shows, the formation of complexes in the melt reduces the conductivity by a factor of 10000 [12]. Here the conductivity is comparable to that of salt melts (3 Ω^{-1} cm^{-1} for CsAu and 1 Ω^{-1} cm^{-1} for the CsCl salt melt).

3. The model with structural disorder

Quantum chemistry and chemical thermodynamics have the tools that are needed to answer the questions of where, when, and how many Zintl configurations can form in a metallic melt and what are the binding energies of these configurations. Since melts, by definition, exist at high temperatures, the curves in Figs 4 and 7 should not be considered a demonstration of metal–insulator transitions. To bring these materials into the realm of objects described by the theory of metal–insulator transitions, they should be quenched by transforming them into glass. Then, for example, the low-temperature dependence of the transport characteristics can, probably, be used to determine the quantitative parameters of the electron traps. So far nothing is known of any attempts to quench such melts with a view to investigating their low-temperature properties.

At the same time, it is true that localization undoubtedly occurs when component concentrations are stoichiometric. Therefore, when discussing the results of experiments in this area of research, it seems appropriate to use the concepts and models developed for describing metal–insulator transitions.

Earlier we mentioned the most common model of regularly arranged potential wells of different depths, or the Anderson model. Each well is formed because of the potential of an impurity atom — donor or acceptor. For the levels in the wells to form a continuous band, the wells must be arranged against a background of smooth random fields, say, the electric fields of charged acceptors or donors with partial compensation of impurities (see Chap. 3 in Ref. [13]). Such broadening of a level into a band may be called classical (Fig. 8).

The alternative of the Anderson model, for the description of a transition in a system of noninteracting electrons that is initiated by a change of disorder, is the model with structural disorder. Here the random potential is built from identical but randomly distributed wells each of which contains a level E_0,

$$V(\mathbf{r}) = \sum_{\mathbf{R}_i} v(\mathbf{r} - \mathbf{R}_i)\,, \tag{9}$$

with the disorder determined by the randomness of the set of vectors $\mathbf{R}_i$. The model contains no classical random fields. Despite the fact that all the wells are identical, the level E_0 in this model also broadens into a band. The broadening is caused by the quantum interaction of the wells due to the overlap of their wave functions [14].

We now break down all the wells into the pairs of nearest neighbors. If the distance between the wells in such a pair is r_{12}, then, since the wells are resonant, i.e. the unperturbed values of the level energy are the same, the overlap of the tails of the wave functions transform the levels into two common split levels with energies

$$E_{1,2} = E_0 \pm \varepsilon_{\mathrm{res}}\,, \qquad \varepsilon_{\mathrm{res}} = J_0\,\frac{\exp\left(-r_{12}/\lambda\right)}{r_{12}}\,, \tag{10}$$

with the collective wave functions

$$\psi_{1,2} = \frac{1}{\sqrt{2}}\,(\varphi_1 \pm \varphi_2) \tag{11}$$

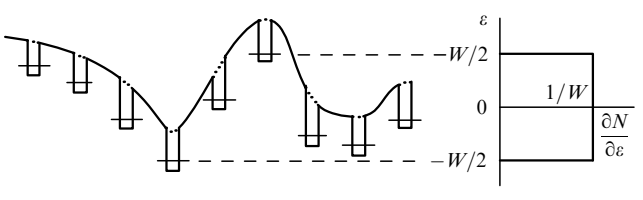

Figure 8. A variant of the realization of the Anderson model: periodically arranged, initially identical potential wells against the background of a smooth random potential (to the right is the model's density of states).

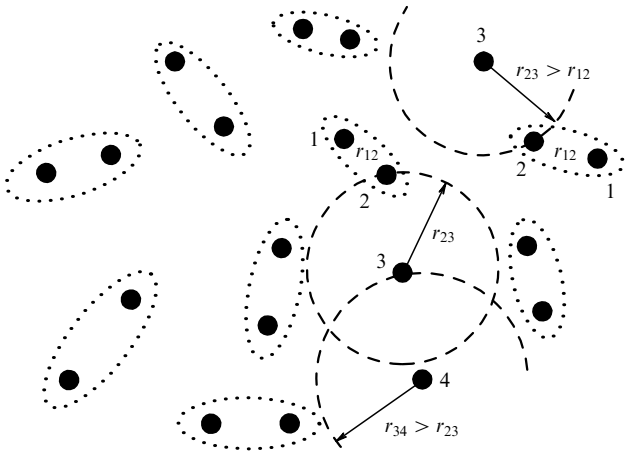

Figure 9. Random arrangement of the impurity wells. Pairs of nearest neighbors are designated by dashed ellipses. Centers labeled 3 adjacent to pairs whose wells are labeled 1 and 2 form triplets with these pairs. One of the triplets enters into a quadruple.

expressed in terms of the unperturbed wave functions φ_1 and φ_2. The quantities J_0 and λ contain the specific characteristics of the wells, the dielectric constant of the material, the effective electron mass, etc. Due to the splitting (10), both levels $E_{1,2}$ are no longer resonant with respect to other neighboring levels, and their interaction with such levels leads to essentially smaller energy shifts

$$\Delta\epsilon \sim \exp\left(-\frac{2r_{s,t}}{\lambda}\right), \qquad s \quad \text{or} \quad t \neq 1,2\,. \tag{12}$$

Figure 9, where the resonant pairs are designated by dotted ellipses, shows that not all centers belong to resonant pairs. For instance, well 2, being the nearest neighbor of well 3, may have well 1 as its nearest neighbor, so that $r_{12} < r_{23}$. Within this triplet, the resonant shifts ε_1 and ε_2 are the biggest, while the shift ε_3 is nonresonant and much smaller, since $\varepsilon_3 \propto \exp(-2r_{23}/\lambda)$. Two such configurations have been depicted in Fig. 9, a triplet and a quadruple in which $r_{12} < r_{23} < r_{34}$. But in triplets and more complicated configurations consisting of four or more wells there is always at least one resonant pair with the smallest well separation and the biggest level shift [14]. Since the characteristic width Δ of the resulting density of states is determined by the resonant well pairs and the average well separation is $n^{-1/3}$, from (10) we obtain

$$\Delta \approx J_0 n^{1/3} \exp\left(-\frac{n^{-1/3}}{\lambda}\right). \tag{13}$$

The tail of the density of states in the region $|\varepsilon| \gg \Delta$ emerges due to the pairs of anomalously close wells with $r_{12} \ll n^{-1/3}$, while states with small $|\varepsilon| \ll \Delta$ emerge due to nonresonant and single wells ([14]; see also Chap. 2 in Ref. [13]). Formula (13) clearly shows that the ratio of the decay length λ to the average distance $n^{-1/3}$ between wells is the main parameter in the model with structural disorder (as it is in the Anderson model)[1].

[1] In the metallic limit $\lambda n^{1/3} \gg 1$, where all the electrons are delocalized and the potential (9) is screened and is only a scattering center, this potential is used in the diffraction theory of electron transport in liquid metals (see Ref. [15]).

The metal – insulator transition in the region where

$$n^{1/3}\lambda \sim 1 \tag{14}$$

has been studied theoretically much less thoroughly in the model with structural disorder than in the Anderson model and, apparently, only numerically (e.g. see Ref. [16]). Still, in this model such a transition undoubtedly exists. Since initially all the ionic traps, or Zintl configurations, are identical, the model with structural disorder seems to be more appropriate for describing them. Each configuration A_4B_4 from (8) is an almost spherical well for the $4 \times 4 + 4 = 20$ valence electrons located inside it on a sequence of energy levels [17]. The decay length λ in Eqn (14) actually refers to the uppermost occupied level. The electrons on deeper levels do not leave the well. This reduces, by a factor of 10, the concentration of potentially delocalizable electrons and facilitates the metal – insulator transition.

Thus, the number of electrons and the level structure in an ionic trap determine by how much the concentration n in the parameter (14) of the model with structural disorder is reduced, while the shape of the well $v(\mathbf{r} - \mathbf{R}_i)$ determines λ. Another control parameter in this model is the magnitude of correlations on the set of vectors $\mathbf{R}_i$: by strengthening the correlations one can change this set from random to regular. The result is shown in Fig. 10 which depicts the change in conductivity of an almost stoichiometric alloy CsAu under crystallization [5, 7]. Here the majority of the wells become resonant and have identical and identically located neighbors. The randomness in the location of the wells is partially retained only to the extent to which the alloy is nonstoichiometric and due to the presence of crystal defects and intercrystalline boundaries. The result of the increase in the number of resonant wells is partial delocalization and a tenfold increase in the conductivity of the crystal compared to that of the melt. However, as Fig. 10 clearly shows, the conductivity of crystalline CsAu is still about 50 times lower than the maximum conductivity $1/\rho^*$ of a standard metal [equation (7)]. Here it is unclear to what extent and how the conductivity depends on deviations from stoichiometry, the number of defects, temperature, and other factors.

4. Quasicrystals

Introducing translational symmetry is not the only way to establish long-range correlations on the set of vectors $\mathbf{R}_i$.

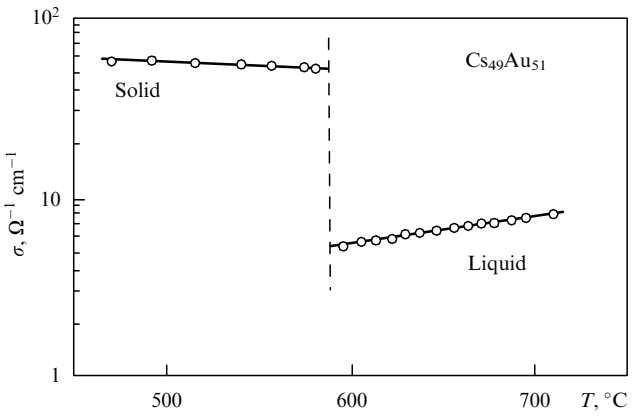

Figure 10. Temperature dependence of the conductivity of the CsAu alloy with 51% of Au in the liquid and solid states [5, 7].

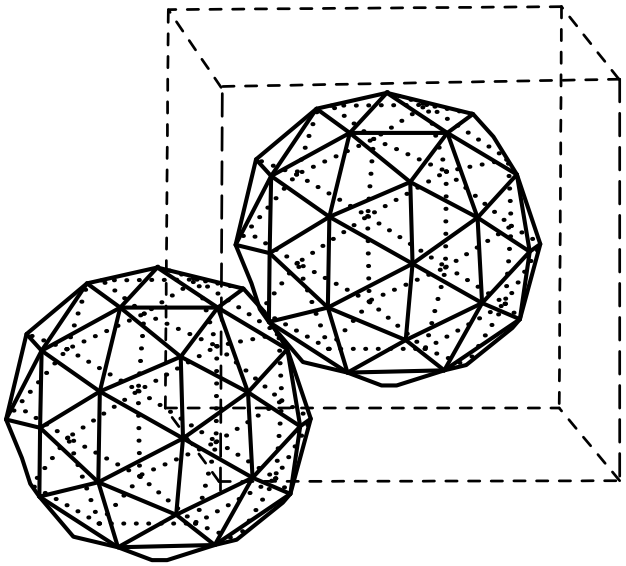

Figure 11. A crystal packing of Mackay icosahedrons, closely resembling a body-centered cubic packing, in the crystalline alloy α(AlMnSi), a quasicrystal approximant [19]. Each icosahedron consists of more than 50 atoms.

Another way to achieve the same result is to introduce quasicrystalline long-range order (Ref. [18]).

Translational symmetry, always present in crystals, allows for the existence of axes of 2-, 3-, 4-, and 6-fold symmetry only. All the same, it is easy to imagine that, of all possible local configurations of a small number of atoms, $A_nB_mC_p$, of the chemical elements A, B, and C, the configuration with the lowest energy has a different symmetry axis, say the axis of 5-fold symmetry. Formation of a crystal from a material with the composition $A_nB_mC_p$ then may proceed in different ways. Sometimes optimal local symmetry is sacrificed, so that a crystal with a different configuration of the nearest neighbors of each atom is formed, with the loss in local configurations energy balanced by gain caused by translational symmetry. There is, however, another possibility. Let us arrange optimal configurations of $n+m+p$ atoms at the sites of a crystal lattice, say, a body-centered cube, as in Fig. 11. Then the loss in energy is caused by mismatch and distortions in the places where these configurations meet, where the short-range order is sure to be nonoptimal. Nevertheless, some substances have such crystal structures. They are called crystal approximants or crystal prototypes of quasicrystals [19].

It occurs, however, that we can do entirely without translational symmetry by densely packing the space with optimal configurations. That this is possible is demonstrated by the Penrose tiling in the lower part of Fig. 12; the plane is covered perfectly (i.e. without gaps and overlaps) by rhombic tiles of two types, with the acute angles equaling $2\pi/5$ and $\pi/5$. These rhombic tiles are depicted in the upper left corner of the same figure. Since the rhombuses adjoin each other at preassigned vertices, the correctly specified functions $F(\mathbf{r})$ on the rhombuses are not discontinuous at the junctions and form a continuous aperiodic function whose individual segments are repeated in the plane an infinite number of times. In the upper right corner of Fig. 12 the arrangement of the vertices of the rhombuses is depicted to the 1 : 2 scale. Since there is no translational symmetry, it is rather difficult to notice any correlations in this arrangement. However, there is long-range order in this system: the rhombic tiles are

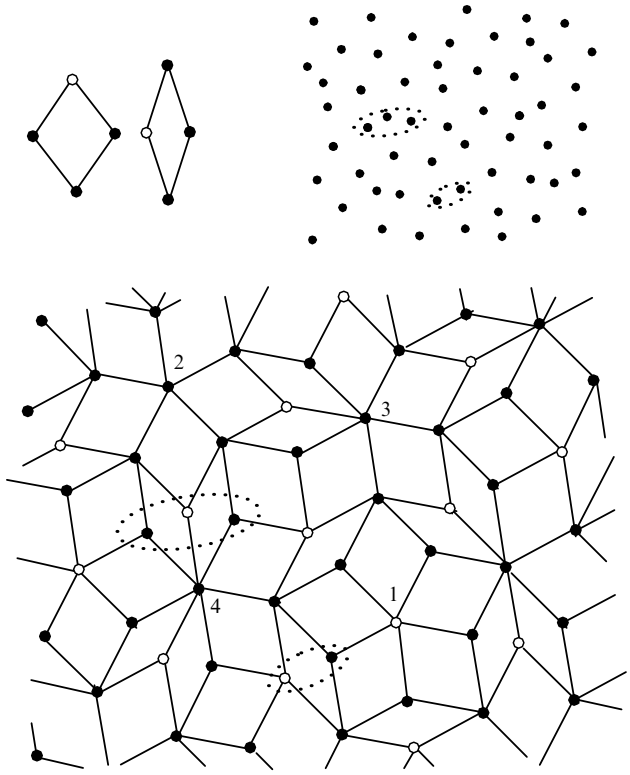

Figure 12. Penrose tiling. Below: tiling a plane without gaps or overlaps by two types of rhombic tiles depicted in the upper left corner of the figure, rhombuses with equal sides a and acute angles $2\pi/5$ and $\pi/5$, respectively (the vertices marked by open circles adjoin each other in the tiling). Upper right corner: the set of rhombus vertices (depicted to the 1 : 2 scale) of the tiling presented in the lower part of the figure. Although each of the sites 1, 2, 3, and 4 has its nearest neighbors only at a distance a, the configurations of these neighbors differ considerably (see the main text). The dotted closed curves mark a resonant pair of closely located sites and a compact triplet of sites.

arranged on the plane in a well-distinguishable pattern (although the pattern is not unique).

Quasicrystals are built according to the same principles. Optimal configurations with high-order symmetry axes are separated by matching spacers in the form of configurations that minimize energy losses at the junctions. The resulting construction has no translational symmetry but has long-range order. Today many families of such materials are known. Most of them are metal alloys in the sense that they consist only of metal atoms: Al–Mn, Ga–Mg–Zn, Al–Cu–Fe, Al–Pd–Re, etc. Here the local base configuration may be extremely complex. For instance, in quasicrystals with the Al–Pd–Mn composition the local base configuration consists of three sells inserted into each other [20]; altogether there are 51 atoms in this configuration (Fig. 13).

Basically, quasicrystals are identified and studied by the X-ray diffraction method, as are ordinary crystals. The Fourier transform of any function of coordinates in a perfect crystal, e.g. the density $\varrho(\mathbf{r})$, is a sum of an infinite number of narrow peaks (ideally, δ-functions):

$$\varrho(\mathbf{r}) = \sum_{\mathbf{q}} \varrho_{\mathbf{q}} \exp(i\mathbf{q}\mathbf{r}) . \qquad (15)$$

The set of $\mathbf{q}$ vectors form a lattice in the $\mathbf{q}$-space with the same symmetry as the initial lattice of atoms. To each site of this reciprocal lattice there corresponds a Bragg reflection in the

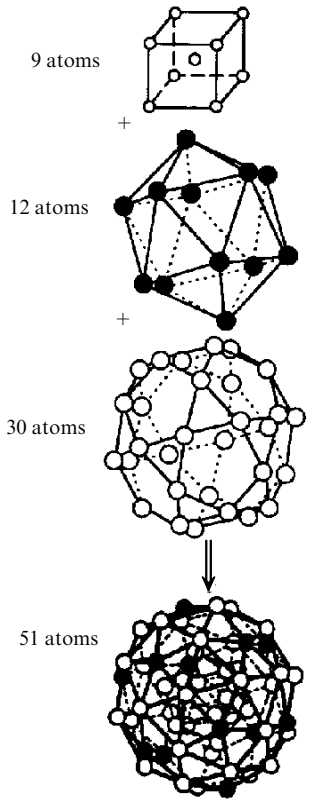

Figure 13. A sequence of shells consisting of atoms in a Mackay pseudoicosahedron which is the base element of the structure of the Al – Pd – Mn quasicrystal; the total number of atoms is 51 [20].

Laue diffraction pattern. The more perfect the crystal the sharper the reflections.

Bragg reflections are not an exceptional property of crystals. For the Fourier transform we can initially take the series (15) in which the set of **q** vectors does not possess translational symmetry. By an inverse Fourier transformation we arrive at a function $\varrho(\mathbf{r})$ that has no translational symmetry either. Such series are the Fourier transforms of quasicrystals. Here the width of the Bragg reflections is still determined by the imperfectness of the structure, namely, by deviation of the local configurations from the ideal configuration, faults of long-range order because of impurities and vacancies, etc. The sharper the Bragg reflections the closer the quasicrystal is to a perfect one.

The following correlation is characteristic of metallic single crystals: the higher the quality of the Laue diffraction pattern of a single crystal of certain substance, the lower the residual resistivity ρ of the crystal. The correlation reflects the wave nature of electrons: the better the conditions for the propagation of an X-ray wave, the smaller the scattering of the Bloch wave. In quasicrystals it is just the opposite: annealing, while increasing the quality of the Laue diffraction pattern, also increases the resistivity. Here the very values of resistivity are extremely high [18]. For instance, in quasicrystals of the Al – Cu – Ru composition at 4 K the resistivity values are as high as 30 mΩ cm, which is approximately 100 times higher than the value of ρ^* estimated by equation (5) from the concentration n of the metallic valence electrons.

The insulating properties manifest themselves most vividly for the Al – Pd – Re system, where the resistivity values at 4 K are stably of order 200 – 300 mΩ cm [18]. Ingots of this alloy can be made by arc melting of a mixture of extremely pure Al, Pd, and Re in an atmosphere of pure argon. After being annealed in vacuum for 24 hours at 980 °C the alloy becomes an icosahedral quasicrystal. However, even after this it remains sensitive to low-temperature annealing at 600 °C. Such annealing in the course of one to two hours may double or even triple the resistivity at 4 K, with the quality of the Laue diffraction pattern remaining the same or even growing.

The temperature dependence of the resistivity of $Al_{70}Pd_{22.5}Re_{7.5}$ quasicrystals can be described in exact agreement with the existing theoretical techniques used to describe conduction in the vicinity of metal – insulator transitions in ordinary crystals. Figure 14 depicts the conductivity as a function of $T^{1/3}$ (the four lower curves) or $T^{1/2}$ (the three upper curves) [21, 22]. To distinguish between the various samples and between the various states of a single sample obtained in the low-temperature annealing process, we select the value σ_{10} of conductivity at 10 K as a parameter (the scales along the horizontal axes in Fig. 14 have been selected in such a way that at this temperature the two scales coincide, as they also do at $T = 0$).

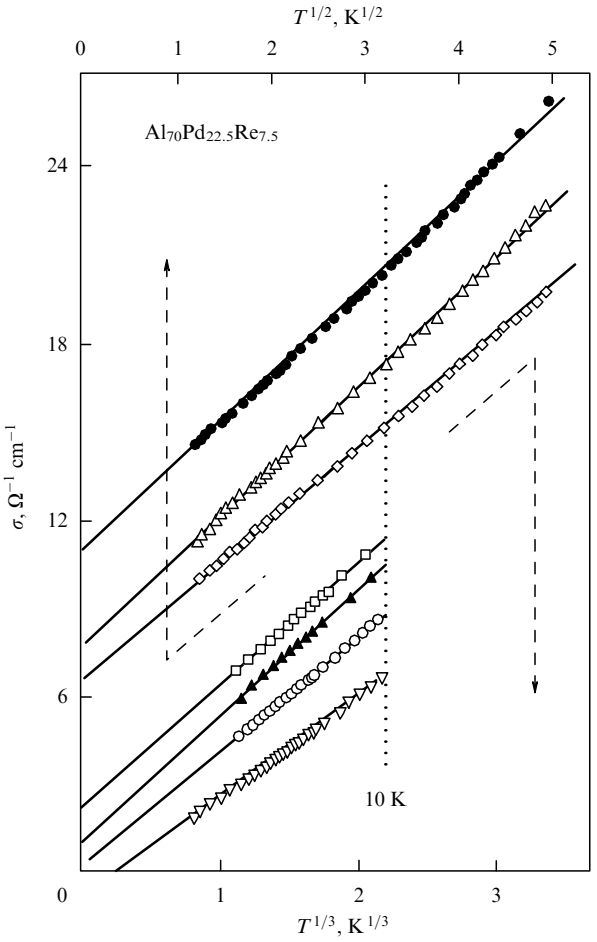

Figure 14. Temperature dependence of the conductivity of the $Al_{70}Pd_{22.5}Re_{7.5}$ quasicrystal. In the immediate vicinity of the metal – insulator transition, the dependence, when represented by a function of $T^{1/3}$, is a straight line (the four lower states). Deep in the metallic region, the dependence becomes a straight line when represented by a function of $T^{1/2}$ (the three upper states). The states can be labeled by the magnitude of the conductivity σ_{10} at 10 K. (The data has been taken from Ref. [21].)

Figure 14 clearly shows that for all measured functions $\sigma(T)$ a linear extrapolation on the selected scales makes it possible to determine $\sigma(0)$ (cf. Ref. [23]). For the tree upper states with $\sigma(0) \gtrsim 6\ \Omega^{-1}\ \mathrm{cm}^{-1}$ we can assume that

$$\Delta\sigma \simeq \sigma_{10} - \sigma(0) \lesssim \sigma(0)\,. \tag{16}$$

This makes it possible to assume that the temperature-dependent part of the conductivity is a quantum correction [24], and this is why in the $(T^{1/2}, \sigma)$ plane the function $\sigma(T)$ is a straight line. For the four lower states with $\sigma_{10} \lesssim (12-14)\ \Omega^{-1}\ \mathrm{cm}^{-1}$ we have the opposite of relation (16). This means that these states are in the critical vicinity of the metal–insulator transition. Hence, when built in the $(T^{1/3}, \sigma)$ plane, the function $\sigma(T)$ is represented by a straight line [24, 25]:

$$\Delta\sigma \equiv \sigma(T) - \sigma(0) \propto T^{1/3}\,. \tag{17}$$

The function $\sigma(T)$ in the critical region in the vicinity of the metal–insulator transition should evolve in this manner (e.g. see Ref. [26]).

Correspondence to ordinary behavior is retained in states with higher resistivities. The extrapolation we have described implies that the metal–insulator transition occurs at $\sigma(10\ \mathrm{K}) \equiv \sigma_{10} \simeq 9\ \Omega^{-1}\ \mathrm{cm}^{-1}$ (open circles in Fig. 14). For states with smaller values of σ_{10} low-temperature transport is realized through the hopping conduction mechanism. That this is actually the case is illustrated by Fig. 15 taken from Ref. [27]. The diagram shows that the conductivity of high-resistance $Al_{70}Pd_{22.5}Re_{7.5}$ quasicrystals obeys Mott's law

$$\ln\sigma \sim T^{-1/4}\,, \tag{18}$$

i.e. these quasicrystals are insulators. Such temperature dependence, $T^{-1/4}$, implies that near the Fermi level the density of states of the electronic spectrum has a constant, finite value.

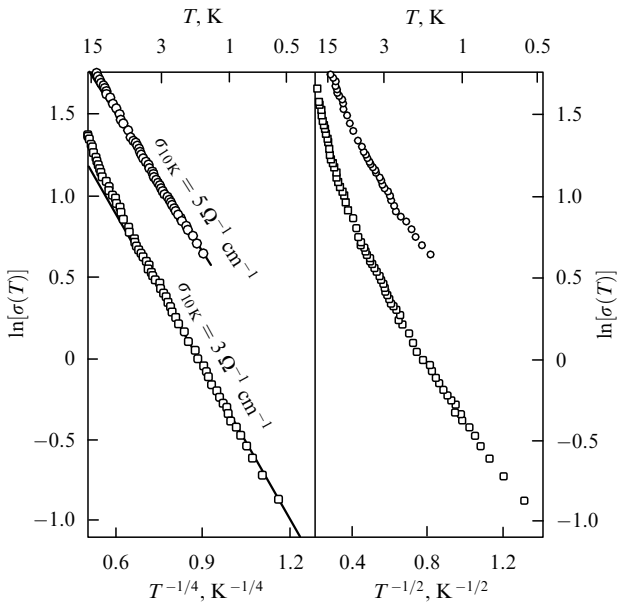

Figure 15. Mott's law for the conductivity of $Al_{70}Pd_{22.5}Re_{7.5}$ quasicrystals in the insulator region (the conductivities at 10 K are 5 and 3 $\Omega^{-1}\ \mathrm{cm}^{-1}$). The dependence becomes a straight line only when $\ln\sigma$ is built as a function of $T^{-1/4}$ [27].

Thus, everything that happens with $Al_{70}Pd_{22.5}Re_{7.5}$ quasicrystals under low-temperature annealing which *improves* conditions for the propagation of X-ray electromagnetic waves, fully corresponds to the pattern of metal–insulator transitions as the parameter $n^{1/3}\lambda$ decreases.

Although the tendency of the resistivity to increase as the Bragg reflections get narrower is a characteristic feature of many families of quasicrystals, so far the metal–insulator transition has been observed only in the Al–Pd–Re system. The maximum resistivity values at 4 K for the systems Al–Cu–Fe, Al–Cu–Ru, and Al–Cu–Mn are smaller than the value for Al–Pd–Re by factor of 10 to 100. Note that even these values are higher than ρ^* calculated by formula (7) by a factor of 10 to 100.

Let us try to understand what is the structure of the $Al_{70}Pd_{22.5}Re_{7.5}$ insulator. Among high-resistivity quasicrystals, the $Al_{70}Pd_{22}Mn_8$ system is the most thoroughly studied one and its structure differs from the structure of $Al_{70}Pd_{22.5}Re_{7.5}$ in only one aspect, i.e. the Re atom is replaced with isovalent Mn. The quantitative characteristics of these quasicrystals can be assumed to be the same.

Thus, the structure of the $Al_{70}Pd_{22}Mn_8$ and $Al_{70}Pd_{22.5}Re_{7.5}$ quasicrystals is based on high-symmetry, close-to-spherical, configurations consisting of 51 atoms (see Fig. 13). According to the diffraction data, the number density of the atoms in these substances is close to $6 \times 10^{22}\ \mathrm{cm}^{-3}$. Since the atoms of the transition elements 'grab' some of the three valence electrons of aluminum, the number of the remaining 'potentially metallic' electrons is somewhat smaller than two per atom, i.e. about $10^{23}\ \mathrm{cm}^{-3}$. For a substance with such a huge electron concentration to be an insulator, the electrons must reside in deep potential wells, or traps. In intermetallic binary melts the traps are configurations of type (8), while in quasicrystals they are the high-symmetry configurations of Fig. 13, which have levels for about 90 of the former valence electrons [20]. Under favorable condition only one to two electrons from the upper levels may leave a trap. Hence, initially the electron configuration is reduced by a factor of 100, after which the more or less standard models describing the metal–insulator transition can be employed.

The arrangement of the levels in all atomic configurations that are traps is, in the zeroth approximation, the same. If the configurations were arranged periodically, the levels would become (in accordance with band theory) bands and the electrons from the upper levels could become delocalized. However, in a quasicrystal there are many ways in which the neighboring configurations can be arranged in relation to a given configuration. According to the model with structural disorder, to each variant of the surroundings there corresponds a specific shift of the levels in the given configuration. Let us explain this using Penrose tiling as an example, for which we turn to Fig. 12. The distance between a given site and a neighboring site can be equal to the length a of the rhombus side or to the length of the smaller diagonal of the narrow rhombus, $a_1 = 0.62a$, or to the length of the smaller diagonal of the wide rhombus, $a_2 = 1.18a$. However, the number of variants of the surroundings which determine the shift of the level of a specific site, is very large. For instance, neighboring sites separated by a distance a_1 may form either pairs or triplets. Sites 1 and 2 each have five neighbors at a distance a, but all five neighbors of site 1 enter into resonant pairs or compact triplets with pairwise distances $a_1 < a$, while site 2 has no such neighbors; site 3 has six neighbors at a

distance a, but three of these neighbors form a compact triplet; site 4 has seven neighbors at a distance a, but six of these neighbors form two compact triplets; etc. As a result, a single level, which initially was the same for all configurations (sites), becomes a band. Whether or not the states in this band are localized depends on the parameter (14), where λ is the decay length of the wave function outside the configuration well.

The very fact that the conductivity of $Al_{70}Pd_{22.5}Re_{7.5}$ is so small is, apparently, caused by the specific combination of the parameters of the configuration well, which makes the decay length λ smaller than in other quasicrystals. In the event of low-temperature annealing of $Al_{70}Pd_{22.5}Re_{7.5}$, the configuration wells in the quasicrystal probably undergo 'internal repair' accompanied by a decrease in the leakage of the wave function from the well, i.e. a decrease in the effective decay length λ.

5. Conclusions

Processes that form the electronic spectrum in two-component melts with an alkali metal as one of the components and in quasicrystals have proved to be very similar. In such systems the effective carrier concentration decreases and the screening weakens, which makes an ordinary metal – insulator transition possible.

The overall scheme is as follows. Suppose that each configuration contains N valence electrons. The potential generated by the ion cores of the atoms in a configuration is so strong, i.e. the potential well is so deep, that the electronic spectrum of these N electrons becomes radically transformed, so that the electrons occupy 'positions' on a ladder of levels. Only one or two electrons on the upper levels have a chance of leaving the well. As a result, the concentration of 'potentially delocalizable' electrons becomes of order n/N, where n is the concentration of the 'initially metallic' valence electrons. In two-component melts, N is of order 10, while in quasicrystals it is of order 100. Thus, the metal – insulator transition occurs in a system with a reduced carrier concentration.

The same line of reasoning can be formulated differently if we imagine each configuration as being a quantum dot in 3D space. The concentration of such dots is of order n/N, with each dot containing N electrons. When one electron leaves a quantum dot, the dot's charge increases by e, and the energy needed to remove the electron is of the order

$$\varepsilon_e \approx \frac{e^2}{r}\,, \tag{19}$$

where r is the radius of the quantum dot. This quantity is similar to the Hubbard energy in the theory of Mott's transition [2]. At the same time, e^2/r is the Coulomb energy of an isolated metal sphere of radius r carrying charge e or the energy of the capacitor that appears in the theory of the Coulomb blockade in nanostructures. On the metal side of the metal – insulator transition, the electric field of a charged dot is screened and the energy (19) is insignificant. On the insulator side there is no screening by free carriers, and the number of charged quantum dots is determined by comparing the energy (19) with the temperature. When $\varepsilon_e \ll T$, the number ν of charged dots is exponentially small:

$$\nu = \frac{n}{N}\exp\left(-\frac{\varepsilon_e}{T}\right). \tag{20}$$

Since conduction in these conditions is determined by tunneling between charged and uncharged dots, ν acts as the number of carriers. This standard line of reasoning used to describe granulated metals determines the activation nature of the conduction [28].

The importance of replacing n with n/N can be illustrated by the fact that when an amorphous alloy is transformed by annealing into a quasicrystal, its resistivity often increases severalfold [18]. Localization is also substantially enhanced by the absence of translational symmetry and of universal short-range order in the mutual arrangement of configurations. Irregularity in this mutual arrangement prevents resonant tunneling. Of course, the presence of translational symmetry by itself cannot guarantee metallic conduction. This is obvious from Fig. 1, where a Mott transition is possible even at $W = 0$. Near the limiting values of concentrations, $n \gtrsim n_{\mathrm{Mott}}$, disorder is essential. Indeed, when the CsAu alloy crystallizes, its resistivity decreases by a factor of 10 (see Fig. 10).

Thus, the two classes of condensed media, briefly discussed in this paper, provide an affirmative answer to the question posed at the end of the Introduction: It is possible to localize a system of valence electrons in a medium consisting only of metal atoms. Such localization is realized through the formation of molecule-like configuration at least in two cases: in two-component melts with an alkali metal as one of the components, and in quasicrystals.

References

1. Anderson P W *Phys. Rev.* **109** 1492 (1958)
2. Mott N F *Metal–Insulator Transitions* 2nd ed. (London: Taylor & Francis, 1990) [Translated into Russian from the 1st ed. (Moscow: Nauka, 1979)]
3. Edwards P P, Sienko M J *Phys. Rev. B* **17** 2575 (1978)
4. Mooij J H *Phys. Status Solidi A* **17** 521 (1973)
5. Hensel F *Adv. Phys.* **28** 555 (1979)
6. van der Lugt W, Geerstma W *Can. J. Phys.* **65** 326 (1987)
7. Schmutzler R W et al. *Ber. Bunsenges. Phys. Chem.* **80** 107 (1976)
8. Calaway W F, Saboungi M-L *J. Phys. F: Met. Phys.* **13** 1213 (1983)
9. Meijer J A, Vinke G J B, van der Lugt W *J. Phys. F: Met. Phys.* **16** 845 (1986)
10. Xu R, de Jonge T, van der Lugt W *Phys. Rev. B* **45** 12788 (1992)
11. van der Lugt W *Phys. Scripta* **T39** 372 (1991)
12. Hoshino H, Schmutzler R W, Hensel F *Phys. Lett. A* **51** 7 (1975)
13. Shklovskiĭ B I, Efros A L *Elektronnye Svoĭstva Legirovannykh Poluprovodnikov* (Electronic Properties of Doped Semiconductors) (Moscow: Nauka, 1979) [Translated into English (Berlin: Springer-Verlag, 1984)]
14. Lifshitz I M *Usp. Fiz. Nauk* **83** 617 (1964) [*Sov. Phys. Usp.* **7** 549 (1965)]
15. Ziman J M *Philos. Mag.* **6** 1013 (1961)
16. Ching W Y, Huber D L *Phys. Rev. B* **25** 1096 (1982)
17. de Heer W A et al., in *Solid State Physics* Vol. 40 (Eds F Seitz, D Turnbull) (New York: Academic Press, 1987) p. 93
18. *Physical Properties of Quasicrystals* (Springer Series in Solid-State Sciences, Vol. 126, Ed. Z M Stadnik) (Berlin: Springer, 1999)
19. Goldman A I, Kelton R F *Rev. Mod. Phys.* **65** 213 (1993)
20. Janot C *Phys. Rev. B* **53** 181 (1996)
21. Wang C-R, Lin S-T *J. Phys. Soc. Jpn* **68** 3988 (1999)
22. Wang C-R, Su T-I, Lin S-T *J. Phys. Soc. Jpn* **69** 3356 (2000)
23. Delahaye J, Berger C *Phys. Rev. B* **64** 094203 (2001)
24. Altshuler B L, Aronov A G, in *Electron–Electron Interactions in Disordered Systems* (Modern Problems in Condensed Matter Sciences, Vol. 10, Eds A L Efros, M Pollak) (Amsterdam: North-Holland, 1985) p. 1
25. Imry Y *J. Appl. Phys.* **52** 1817 (1981)
26. Gantmakher V F et al. *Zh. Eksp. Teor. Fiz.* **103** 1460 (1993) [*JETP* **76** 714 (1993)]
27. Wang C R et al. *J. Phys. Soc. Jpn* **67** 2383 (1998)
28. Abeles B et al. *Adv. Phys.* **24** 407 (1975)